8

Hollow atom formation on an insulator surface

This chapter presents KLL Auger spectra of hydrogenic (1s) N, O, and Ne ions impinging on an insulating LiF(100) single crystal surface. The beam energy and incident angle have been varied such that the lowest possible velocity towards the target is achieved, while at the same time the velocity parallel to the target is varied by a factor of 10. Similarities and differences between the LiF spectra and spectra measured on (semi) conducting Si(100) and Al(110) surfaces are discussed.

8.1 Introduction

In the previous chapters a detailed model has been developed *de facto* describing the last deexcitation step (the filling of the K-shell vacancy by emission of a KLL Auger electron) of hollow atoms formed in front of *conducting* surfaces. The role of Coster-Kronig transitions quenching the numerous "hollow atom" states into a limited number of "KLL-Auger" states and the processes accounting for the filling of the energetic L-shell vacancies have been highlighted. In this chapter it will be shown that with this model, insight can be obtained into the overall neutralization and deexcitation sequence of multiply charged ions hitting on solid surfaces. This will be done using Auger spectra obtained from multiply charged ions impinging on an *insulating* surface.

For an insulator, the first steps of ion surface interaction might already be quite different as compared to a conducting surface. Delocalized electrons are not as abundantly available as in a metal, and their binding energy ("effective work function") is much larger than in a metal. Since, according to the overbarrier model,[130] the distance of first electron capture is proportional to the inverse of the target work function W_ϕ, electrons will be captured much closer to the surface for an insulator. Moreover, capture of more than one (localized) electron from a single target site is unlikely since that would imply an even larger binding energy to overcome. Therefore, in order to achieve complete projectile neutralization, electrons have to be captured from different, maybe adjacent lattice sites. This implies a difference in the neutralization dynamics for different experimental settings. For instance, an energetic, grazingly incident projectile "probes" many lattice sites on its trajectory whereas a slow ion, impinging perpendicularly on the insulator surface only probes few electron donor sites. In the former situation complete neutralization is obviously more probable than for the latter one.

8.2 Experiments

In order to investigate highly charged ion interaction with an insulating surface we have measured energy spectra of KLL Auger electrons resulting from collisions of hydrogen-like N^{6+}, O^{7+}, and Ne^{9+} ions on the LiF(100) surface. LiF is an insulator, however at elevated temperatures it exhibits an ionic conductivity which is sufficient to avoid charging up induced by impact of low intensity ion beams (several tens of nA).

Figure 8.1 shows energy spectra resulting from collisions of N^{6+} ions on the LiF surface. Electrons in the energy range between 320 and 400 eV are due to KLL Auger processes. For comparison similar spectra shown

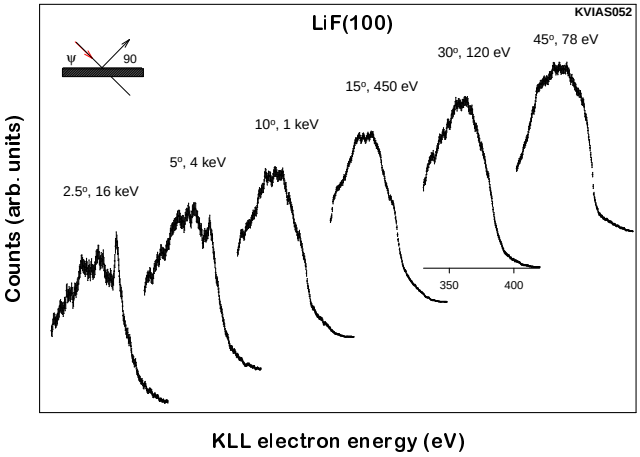

FIGURE 8.1: *KLL Auger spectra of N^{6+} on LiF(100). The beam energy E_0 and incident angle ψ have been varied such to that $v_\perp$ is kept constant. The ordinate is linear.*

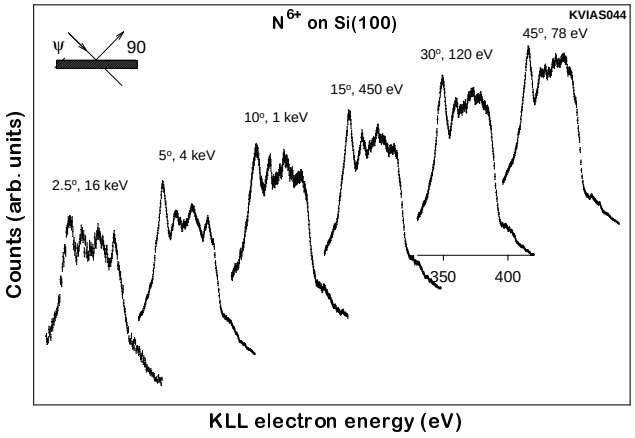

FIGURE 8.2: *KLL Auger spectra of N^{6+} on Si(100) (see chapter 7). Beam energy and incident angle similar to figure 8.1.*

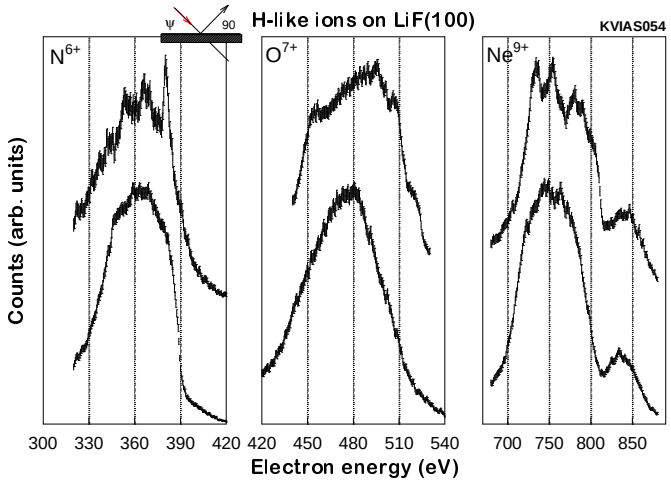

FIGURE 8.3: *KLL Auger spectra of N^{6+}, O^{7+} and Ne^{9+} on LiF(100), Energy/incident angle: 16 keV/2.5° (top) and 100 eV/45° (bottom).*

previously in figure 7.1 of chapter 7 of N^{6+} on the Si(100) surface are also shown (figure 8.2). In figure 8.3 KLL Auger electron distributions are shown for N^{6+}, O^{7+}, and Ne^{9+} impinging on the LiF surface.

For obtaining the various spectra the collision energy and the angle of incidence have been varied simultaneously. This way the velocity towards the surface $v_\perp$ and thereby the timescales governing above surface neutralization and deexcitation, remained constant for all measurements. In order to maximize the time spent by the projectiles in front of the surface, the projectile energy towards the surface was taken as small as possible, without loosing too much beam intensity. Under these experimental conditions the vertical velocity is close to its principal lower limit, given by the image charge acceleration which is also active for LiF (see e.g.[131] and chapter 2).

8.2.1 The N^{6+} series

In comparing the series of measurements depicted in figures 8.1 and 8.2, two striking features are observed. Firstly, the $1s : 2s^2\,3l^4$ peak which shows up at the low energy side of the KLL spectra for the Si target, is missing for LiF whereas for both targets the sharp ($\Delta E \leq$ 2eV FWHM) $1s\,2s^2 2p^4$ peak comes up at the high energy side (∼382 eV) of the spectra with increasing collision energy. Secondly, the low energy slope of all KLL Auger peaks measured on the LiF target exhibits a remarkable shift by 10-15 eV towards

lower energies, as compared to the Si target, whereas the high energy peak is practically at the same energy (382 eV) for both targets.

The experimental results can be interpreted in a straightforward way by the L-shell filling model developed in chapter 7. In this model, basically two processes account for the filling of the L-shell vacancies. At first, a slow mechanism starts as soon as the hollow atom is formed and proceeds mainly via LVV type Auger cascades together with resonant electron capture from and loss to the target. Initially, the L-shell filling rate $\Gamma_L(r)$ is much smaller than the KLL Auger rate Γ_K. Consequently, as soon as two electrons have reached the L-shell, KLL-decay is much more likely than a further accumulation of L-electrons via Auger processes. Therefore this mechanism gives predominantly rise to KLL processes with a doubly filled L-shell, resulting in the low energy part of the measured spectra. Apparently this mechanism is active for the Si(100) (and Al(110), see chapter 7) target and gives rise to the sharp peak at 350 eV. For LiF however, L-shell filling by LVV Auger processes contributes only weakly. Moreover, the projectiles seem to be incompletely screened in front of the LiF surface. The broadening of the low energy slope in the spectra and the shift towards lower energies can be ascribed to KLL electron emission from such differently screened projectiles, as was shown in figures 5.3 and 5.3 of chapter 5.

The second, fast mechanism for L-shell population caused by a direct transfer of target core electrons becomes active at small internuclear distances. The localized nature of this type of vacancy exchange leads to a velocity (or "collision frequency") dependent filling rate $\Gamma_L(r) = P_L(r)v/d$. For sufficiently high collision frequencies (i.e. v/d of the order of 10^{15}/s) a further accumulation of electrons in the L-shell up to the maximum is always more likely than a KLL decay from an incompletely filled L-shell. The rise of the sharp $KL_{2,3}L_{2,3}$ peak at 382 eV corresponding to decay from a filled L-shell, with increasing velocity, is observed for both targets. This can be taken as clear evidence for such a fast filling mechanism to be active in the collisions considered here.

8.2.2 The N, O, Ne series

The magnitude of the LVV Auger rate $\Gamma_L^A(r)$ is to a large extent determined by target properties (free electron density, work function) and does not vary too much for the ions used here.[132] However, cross sections for *direct* filling of L-vacancies by target core electrons are very sensitive to the binding energies of the target and projectile levels involved.[133, 134] This is reflected in the spectra depicted in figure 8.3; for small projectile energies the projectiles' L-shell is mainly filled by slow LVV processes giving similar distributions for N, O and Ne. So apparently for all three ion species the above surface contributions are comparable. But the 16 keV spectra taken at grazing

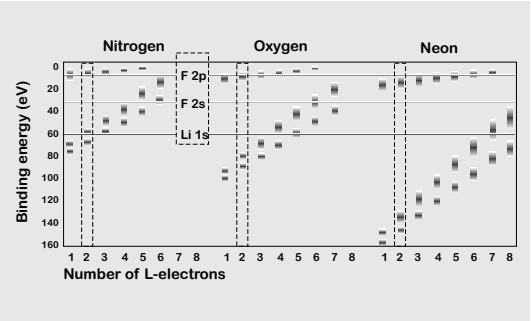

FIGURE 8.4: *L and M electron binding energies for N, O and Ne hollow atom configurations* $1s2l^x3l^{Z-x-1}$ *as a function of* x*, the number of L-electrons present. Also shown are the F* $2p$*,* $2s$ *and Li* $1s$ *binding energies in LiF.*

incidence show a remarkable behavior: the rise of the sharp peak at the high energy side for N^{6+} is absent for O^{7+} and Ne^{9+}. For O, some structure shows up at both sides of the spectrum, and for Ne, the typical KL_1L_1 and $KL_1L_{2,3}$ peaks arising from decay with only *two* L-electrons as discussed before, come up. Secondly, only for Ne, a significant contribution of KLM Auger electrons is observed in the spectra. Inspection of the binding energies of L- and M-shell vacancies for N(1s) and Ne(1s) projectiles depicted in figure 8.4 shows that for N(1s), the L-shell vacancies are quasi-resonant with F 2s and 2p electrons ($E_b \simeq 35$ and $\simeq$12 eV respectively) and with Li 1s electrons (at $\simeq$62 eV).[135] Resonant transfer of F 2p electrons into N(1s) M-shell vacancies seems unlikely since these have binding energies of less than 10 eV.

However, for Ne(1s), the situation is different. The binding energies of L-shell vacancies is of the order of 150 eV, for an empty L-shell, to 40 eV, for a 2p electron in a filled L-shell. The M-shell vacancies are bound with $\simeq$20 eV for an empty L-shell to about 10 eV for an almost filled L-shell. So, for low L-occupancy, quasi-resonant transfer of core electrons from LiF to Ne(n=2) is blocked. But efficient transfer of F 2p electrons into Ne(n=3) is possible. So, for large collision frequencies, the Ne(1s) M-shell is filled up efficiently, after which the filling rate of the Ne L-shell is simply given by the Ne(1s) LMM rate. So for large collision frequencies a well defined, neutral $Ne(1s2l^x3l^{9-x})$ hollow atom is formed giving rise to the well known Auger spectrum.

For O(1s), the situation is most complicated. Initially, M-shell vacancies are resonant with F-2p electrons, and filling of L-shell vacancies is blocked. However, as soon as 3 or 4 L-electrons are present, further filling by direct

capture becomes possible. But then the M-shell vacancies become unbound. So, for sufficiently high energies the O(1s) KLL Auger consists of contributions from states with few L-electrons (which accumulated via LMM/LVV Auger decay) and of states with a filled L-shell. It should be noted here that KLL emission from a $O(1s2l^8)^-$ *negative* ion is energetically allowed.

8.3 Discussion

The most remarkable features of the LiF KLL Auger spectra, i.e. the absence of structure and broadening observed for small energies, can in principle be explained by assuming that under such conditions the formation of a neutral, hollow atom is strongly inhibited. For low collision energies, KLL emission takes place from insufficiently screened projectiles leading to smearing of structure and broadening of the spectra towards lower energies. But for large energies and grazing incidence, complete neutralization – by quasi resonant capture of LiF core electrons during close collisions – is achieved before KLL emission occurs. Reduced projectile deexcitation in front of a LiF surface has also been inferred from total electron yield measurements.[136]

The comparison between spectra of LiF and those of the Si (and Al, see the previous chapter) target sheds new light on the question to what extent KLL electron emission really takes place above the surface for conducting targets. For high collision frequencies, L-shell filling by close ion-surface atom collisions is faster than KLL decay. This results in a rapid filling of the L-shell up to its maximum before KLL decay occurs. Decay with only two L-electrons present becomes unlikely as soon as the projectile suffers these rapid close collisions.

At least for the 16 keV spectra, Auger emission with two L-electrons present (contributing to the low-energy peaks) will be negligible after the "close collision" range has been entered. The observed intensity of the KL_1L_1 and $KL_{2,3}L_{2,3}$ in case of 16 keV N^{6+}-Si collisions can therefore completely be ascribed to *above-surface* emission. This intensity is practically constant for all the spectra taken at constant *vertical* velocity while the *parallel* velocities are varied by a factor of 10. This supports the view that the peak is always due to emission before close collisions occur.

Finally, the absence in the 'LiF spectra' of the peaks due to above-surface emission leads to the conclusion that formation of highly excited, hollow atoms in front of such an insulating LiF target is much less probable than in front of metal and semiconductor targets.